Experimental Observation of Strong Photon Localization
in Disordered Photonic Crystal Waveguides

J. Topolancik,[1] B. Ilic,[2] and F. Vollmer[1,*]

[1]*Rowland Institute at Harvard, Harvard University, Cambridge, Massachusetts 02142, USA*
[2]*Cornell Nanofabrication Facility, Department of Applied Physics and Field of Biophysics, Cornell University,
Ithaca, New York 14853, USA*
(Received 19 April 2007; revised manuscript received 16 October 2007; published 19 December 2007)

We demonstrate experimentally that structural perturbations imposed on highly dispersive photonic crystal-based waveguides give rise to spectral features that bear signatures of Anderson localization. Sharp resonances with effective Q's of over 30 000 are found in scattering spectra of disordered waveguides. The resonances are observed in a ~20-nm bandwidth centered at the cutoff of slowly guided Bloch modes. The origin of the spectral features can be explained by the interference of coherently scattered electromagnetic waves which results in the formation of a narrow impurity (or localization) band populated with spectrally distinct quasistates. Standard photon localization criteria are fulfilled in the localization band.

Transport of waves through a medium can be severely suppressed and even halted by interference and multiple scattering from random impurities which can give rise to strong (or Anderson) localization [1–3]. The theory behind the process was originally developed for matter waves (electrons in disordered atomic crystals) [1], but it can be directly extended to classical waves where the verification of its universal principles is not complicated by Coulomb and electron-phonon interactions [2,3]. In this regard, random scattering media [4–7] and disordered lattices [8] have attracted considerable experimental interest as promising model systems for testing the localization concepts on electromagnetic waves and light, in particular. Experimental demonstration of strong photon localization is rather difficult to achieve as it requires strongly-scattering materials with minimum absorption. Several groups have reported experimental signs of localization transitions in random media [6,7] and, more recently, in a disordered two-dimensional (2D) lattice [8]. It has been proposed by John [9] that the localization conditions should be easier to fulfill in high-index-contrast periodic structures with a photonic band gap (PBG) [10]. To our knowledge, this idea has been tested successfully only in metal-wire networks at microwave frequencies where absorbing materials complicate interpretation of results as it is difficult to distinguish absorption from localization [11]. In this Letter, we report direct experimental observations of localized electromagnetic fields in nonabsorbing, geometrically-disordered photonic crystal (PhC) structures at optical frequencies.

High-refractive-index slabs with 2D arrays of airholes exhibit large PBGs for the TE-like polarization (**E**-field parallel to 2D-plane) [12], which established them as a popular platform for designing waveguides [13–15] and nanocavities [16–18]. Engineered PhC nanostructures guide and confine light remarkably well by relying on Bragg reflections in the 2D-plane and on total internal reflection in the out-of-plane direction. Guiding losses

and cavity quality (Q) factors are believed to be limited primarily by the fabrication-induced surface roughness which breaks the PhC periodicity and destroys the Bloch-wave coherence by diffusive scattering. Considerable efforts have thus been expended to improve fabrication processes which, together with the progress in design optimization, have produced highly dispersive (or slow-light) waveguides [19,20] and optical nanocavities with ultrahigh Qs and record-low modal volumes [21,22]. Here, we show experimental evidence that random departures from index periodicity need not necessarily set off decoherence, but can produce a fundamentally different type of coherent localization analogous to that observed in strongly scattering random media [4–7]. More specifically, we will argue that scattered spectra collected from geometrically disordered PhC waveguides in freestanding silicon slabs bear signatures of Anderson localization.

Disordered PhC structures consisting of a hexagonal lattice of holes were patterned in silicon-on-insulator substrates using electron beam lithography and chlorine-based inductively coupled plasma reactive ion etching. PhCs with various fill factors ($f = R/a$, where R is the effective hole radius and a is the lattice constant) were fabricated. As illustrated in the scanning electron micrograph (SEM) in Fig. 1(b), the fabricated patterns carry a significant geometrical disorder in addition to the usual surface roughness introduced during processing. The positions of the airholes are fixed in an array with a lattice constant $a = 410$ nm; their size is fairly constant with $\delta R/R \sim 1.3\%$, but their shapes differ noticeably from an ideal circle. More specifically, statistical analysis of PhCs investigated here reveals that the root-mean-square deviation of the feature's edge from the radius of the fitted circle (R) is ~6 nm whereas values of ~2 nm have been reported in the state-of-the-art structures fabricated with optimized lithographic and etching processes [22]. The disordered patterns were defined using a high energy (100 kV) electron beam (JEOL 9300) to which deflection jitter was applied. The image analysis
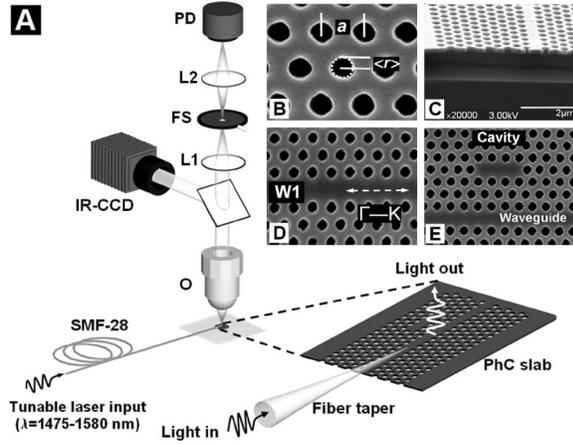
FIG. 1. (a) Schematic of the measurement setup. Vertically
scattered light is collected with an objective (O) and imaged
with a lens (L1) onto a field-stop (FS) consisting of a variable
aperture which selects the field of view. Another lens (L2)
focuses light from the selected area into an IR photodiode
(PD). A beam splitter redirects a fraction of the collimated
beam into an IR charge coupled device (IR-CCD) for imaging.
(b) SEM of a typical disordered PhC pattern; (c) the cross section
of a freestanding W1 PhC waveguide; (d) top image of a W1
waveguide; and (e) example of a donor-defect cavity.

of the patterns fabricated this way did not reveal any
longrange correlations. It will be argued later that the
introduced geometrical perturbations are small enough
not to significantly affect the band structure of the under-
lying periodic lattice (this way the traditional PBG defect
engineering concepts such as band gap, point-defect mode,
line-defect dispersion, etc., still apply), but sufficient to
generate significant multiple scattering of Bloch waves
necessary for strong localization. Once the holes were
etched into the ~210-nm-thick silicon layer, the patterns
were cleaved, and the buried oxide layer was removed with
a buffered hydrofluoric acid solution forming a freestand-
ing PhC slab shown in Fig. 1(c). The inner walls of the
etched holes are smooth and nearly vertical. The disor-
dered PhC enfolds a ~60-μm-long line-defect waveguide
(W1) formed by a row of missing holes along the ΓK
direction of the reciprocal-lattice, surrounded on both sides
by ten rows of holes [see Figs. 1(b) and 1(c)]. Various
donor-defect cavities defined by a single or multiple miss-
ing holes were also patterned in some samples near the
waveguides. An example of a linear, three-defect cavity is
shown in Fig. 1(e).

Coherent light from an infrared (IR) diode laser tunable
from 1475 to 1580 nm was coupled into W1s from a single-
mode optical fiber (SMF-28). To compensate for the sig-
nificant impedance mismatch inherent to conventional end-
fire coupling, PhC modes were excited with a nonlinear
fiber taper. The taper, prepared by pulling a melted fiber
and etching its tip down to the W1 dimensions ($\sqrt{3} \times a$),
was positioned on top of the PhC-slab as illustrated in
Fig. 1(a). The arrangement allows the light to leak out of

the taper and to evanescently couple into the W1 wave-
guide. Tapered silica fibers have been employed in a simi-
lar fashion previously to couple light into waveguides in
PhC slabs [23]. Once excited, the PhC modes propagate in
the waveguide and interact with the adjacent defect cavities
which then emit light vertically out of the slab. This
established approach to trapping and extraction of photons
from PhC lattice defects is known as the surface-emitting
channel drop filter [24]. The emitted light was collected
with an infinity-corrected objective ($100 \times$, NA = 0.80)
and its intensity monitored with an InGaAs photodiode as
the coherent source was scanned. A beam splitter redir-
ected a fraction of the collimated beam to an IR camera for
imaging. A field stop was placed in front of the photodiode
to locally probe 10 μm-long waveguide sections and to
block parts of the free-propagating beam deflected acci-
dentally into the objective from surface impurities.

The spectrum collected from a donor-defect cavity sepa-
rated from W1 by four rows of holes is shown in Fig. 2(a).
It contains two distinct features: an isolated peak at
1492 nm with the Q of ~3000 [Fig. 2(b)], as inferred
from its full width at half maximum linewidth; and a
striking series of extremely sharp ($\Delta\lambda \sim 50$ pm), discrete
peaks in a narrow band centered at ~1570 nm [Fig. 2(d)].
The IR image in Fig. 2(c) indicates that the analyzed light
is emitted primarily from the donor-cavity region. To ex-
plain the origins of the measured spectra, we need to
address the dispersion characteristics of PhC waveguides
and describe how they are affected by disorder. Although it
is possible to systematically study how specific types of
disorder affect transport through waveguides, e.g., by ana-
lyzing ensembles of randomized structures with the finite-
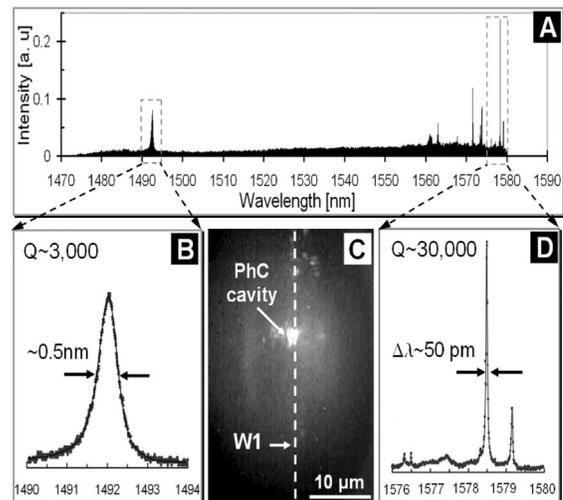difference-time-domain (FDTD) method [25], this would

FIG. 2. (a) Spectrum acquired from a single-defect cavity
separated from the W1 waveguide by four rows of airholes;
(b) 4 nm-wide detailed scan showing the solitary broad feature;
(c) IR image of the collected light; and (d) high-resolution scan
of a 4 nm-wide section of the band containing sharp spectral
peaks.

require unreasonably large simulation domains and unfeasible computation times. Such a methodical treatment of disorder is beyond the scope of this experimental Letter and will be discussed elsewhere. Instead, here we use the established supercell approach and 3D plane-wave expansion [26] to calculate the band structure of line defects in ideal, disorder-free crystals, and qualitatively explain how disorder affects dispersion and gives rise to the observed spectral features. The supercell used to compute the band diagrams is shown in the inset of Fig. 3(a). Its dimensions are $7\sqrt{3}a \times 4a \times a$ and the refractive index of silicon used in the simulations is $n = 3.52$. The simulated slab is $\sim 0.51a$-thick, and the holes are circular with radii that correspond to the fill factors of the fabricated PhCs determined from SEM images. Figure 3(a) shows the projected band structure of a W1 with $f \cong 0.28$. To conceptually show the effect of disorder, we introduce error bars representing uncertainty in the computed eigenfrequencies. Their magnitude in Fig. 3(a) is arbitrary and is merely meant to reflect the severity of disorder, i.e., how much the departures from the holes' roundness affect the band structure. A single nonleaky mode bounded by the light line ($\omega \cong 0.283[a/\lambda]$) and the stop band ($\omega \cong 0.265[a/\lambda]$) falls within the scan range of the probing laser. The mode has an even parity and exhibits anomalous dispersion unique to PhC waveguides [13–15]. Its group velocity ($v_g = d\omega/dk$) gradually decreases as the wave vector approaches the zone boundary (the slow-light regime). We attribute the solitary spectral peak at 1492 nm ($\omega \cong 0.2748[a/\lambda]$) to a point-defect cavity mode excited evanescently by the waveguide in the classical (or index-

guided) regime. Even though the crystal disorder reduces the PBG and degrades the cavity Q, it permits proper waveguiding and Bragg localization. Whereas the isolated resonance can be accounted for with the conventional donor-cavity PBG defect picture [10], we do not believe the sharp peaks at longer wavelengths (in the slow-light regime) can be explained within the simple framework. Instead, we contend here that these features are caused by disorder and are a manifestation of Anderson localization.

Calculated dispersion diagrams of even modes in W1 waveguides with different fill factors: $f = 0.26$, $f = 0.28$, and $f = 0.30$ are presented in Fig. 3(b). The plots indicate that increasing f shifts the mode's edge to higher frequencies. The same trend is observed experimentally for the bands of narrow peaks measured on the fabricated disordered waveguides with equivalent fs [Fig. 3(c)], which suggests that the spectral position of the spectral feature is dictated by the band structure. Our measurements directly probe the spectral characteristics of local fields in the PhC structure by analyzing the light scattered vertically by donor cavities. The cavities are usually off-resonance in the bandwidth where the peaks are present, and they merely enhance the scattering efficiency out of the PhC slab. Distinct Bragg defect modes, such as the one shown in Fig. 2(b), are seldom detected as their spectral positions and Qs depend sensitively on the cavity geometry and disorder generally either degrades the Q or shifts the resonant frequency outside the limited scan range of the probing laser. On the other hand, pronounced narrow spectral features always appear, even in disordered waveguides fabricated without donor cavities. In this case, the sharp peaks are observed, though with a reduced intensity, in arbitrary positions along the probed waveguides. The fea-
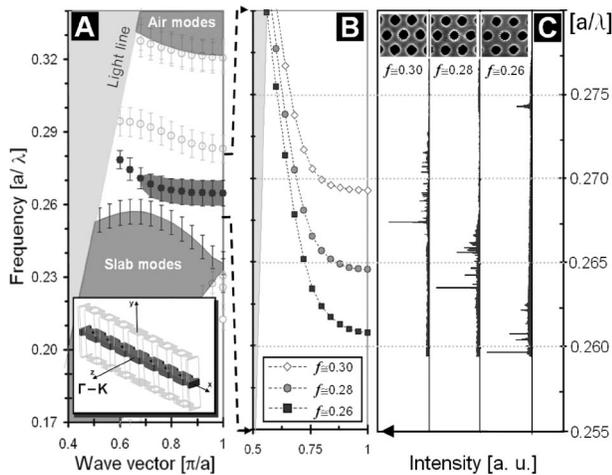

FIG. 3.   (a) Calculated band structure of a W1 waveguide ($f \cong 0.28$) with an even-parity guided mode (black circles). The dark-shaded region around the mode's edge outlines the strong-localization window. The inset shows the supercell used in the plane wave expansion simulations. (b) Calculated dispersion curves for the even mode in waveguides with three different fill factors; and (c) spectra collected from fabricated waveguides with the equivalent fill factors. The insets show the corresponding SEM images of the PhC structures.
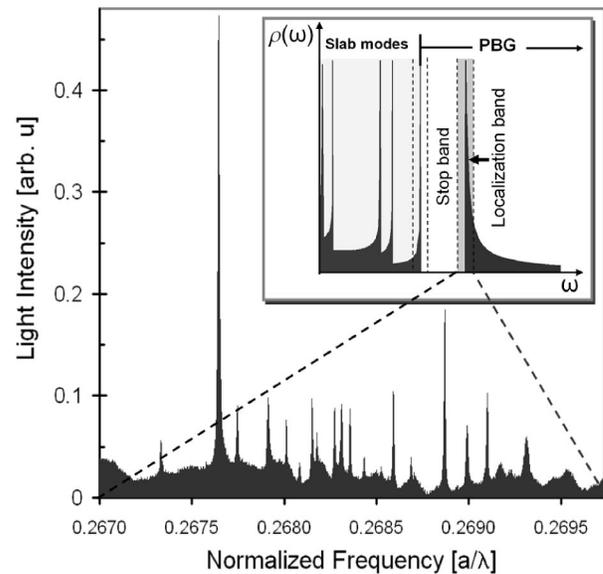

FIG. 4.   Detailed spectrum of the localization band collected from a disordered W1 ($f \cong 0.30$). The inset shows the calculated DOS of a defect-free waveguide. Disorder creates a localization band (gray) around the slow mode's cutoff.

tures are located spectrally in a narrow localization win-
dow in the $k - \omega$ space which is outlined schematically as
a dark-shaded area around the mode's edge in Fig. 3(a). IR
images of the scattered fields indicate that some of the light
is emitted from small areas from which we estimate the
localization lengths of a few lattice constants. A closeup of
the spectrum collected from a section of a disordered W1
with no donor-cavity ($f \cong 0.30$) is presented in Fig. 4. The
scan reveals a band filled with multiple sharp resonances,
rather than a broad spectral feature anticipated as a result of
the increased vertical-scattering loss from the waveguide in
the slow-light regime [27]. While the overall spectral
position of the localized modes is dictated by the mode
structure of the underlying PhC, their line widths and
intensities are shaped by three important structural parame-
ters. The first one is the local dielectric function which
determines the cavity geometry and with it the amount of
the intrinsic leakage out of the slab plane. The second is the
global dielectric function which includes other cavities
along the waveguide through which light can escape in-
plane by resonant coupling. The last parameter is the
extrinsic loss due to unintentional surface roughness and
nonvertical sidewalls which further degrade the cavity Q.

The physical origins of strong localization in disordered
W1s can be explained within the context of theories of
wave propagation in disordered media [28,29]. Slow light
in the highly dispersive waveguides is susceptible to co-
herent backscattering which can block the transport if
certain conditions are met. Introduction of random disorder
fills the edge of the stop band with localized quasistates
creating a string of resonant cavities along the waveguide.
Although disorder-induced broadening of the density-of-
states (DOS) into the stop band of such slow-light struc-
tures has been theoretically predicted and its effect on the
propagation speed around the band edge was investigated
[30], no localization phenomena have been discussed. The
defect states that populate the stop band are well-localized,
i.e., spatially and spectrally distinct, only if their level
spacing ($\Delta\nu$) is large enough and the level widths ($\delta\nu$)
small enough so that the modes do not overlap. This
essentially says that a fundamental localization condition,
the Thouless criterion ($\delta \equiv \delta\nu/\Delta\nu < 1$) [28], is satisfied
as it is clearly the case here. Significantly overlapping
modes would enable transport and destroy localization.
The origin of the localization band is shown schematically
in the inset of Fig. 4. A disorder-free W1 exhibits an abrupt
transition from the guided mode to the stop band, i.e., the
DOS of the guided modes, $\rho(\omega) \propto (v_g)^{-1}$, diverges at the
mode's cutoff beyond which it suddenly vanishes. Disorder
causes band-structure fluctuations that smear the sharp
cutoff creating a transitional (or impurity) band filled
with both slowly guided modes credited to the residual
refractive-index periodicity and localized quasistates aris-
ing from disorder. Light propagation in the band can be
viewed as a combination of remnant waveguiding and
resonant transport. The observed localized quasimodes

with effective Qs of over 30 000 (Fig. 4) are in many
respects similar to the engineered defect- modes in PhC-
heterostructure cavities [21,22] in which periodicity of
PhC waveguides is broken intentionally by locally increas-
ing the lattice constant. These modes have small modal
volumes and record-high Qs of up to $\sim 10^6$. An interesting
question worth exploring is whether random disorder can
confine light with similar efficiency.

---

*vollmer@rowland.harvard.edu
[1] P. W. Anderson, Phys. Rev. **109**, 1492 (1958).
[2] S. John, Phys. Rev. Lett. **53**, 2169 (1984).
[3] P. W. Anderson, Philos. Mag. B **52**, 505 (1985).
[4] R. Dalichaouch *et al.*, Nature (London) **354**, 53 (1991).
[5] A. A. Chabanov, M. Stoytchev, and A. Z. Genack, Nature
(London) **404**, 850 (2000).
[6] D. S. Wiersma *et al.*, Nature (London) **390**, 671 (1997).
[7] M. Störzer *et al.*, Phys. Rev. Lett. **96**, 063904 (2006).
[8] T. Schwartz *et al.*, Nature (London) **446**, 52 (2007).
[9] S. John, Phys. Rev. Lett. **58**, 2486 (1987).
[10] J. D. Joannopoulos, R. D. Meade, and J. N. Winn, *Photonic
Crystals: Molding the Flow of Light* (Princeton University
Press, Princeton, NJ, 1995).
[11] M. Stoytchev and A. Z. Genack, Phys. Rev. B **55**, R8617
(1997).
[12] T. Krauss, R. DeLaRue, and S. Brand, Nature (London)
383, 699 (1996).
[13] M. Lončar *et al.*, J. Lightwave Technol. **18**, 1402 (2000).
[14] S. G. Johnson *et al.*, Phys. Rev. B **62**, 8212 (2000).
[15] M. Notomi *et al.*, Phys. Rev. Lett. **87**, 253902 (2001).
[16] O. Painter, J. Vučković, and A. Scherer, J. Opt. Soc. Am. B
16, 275 (1999).
[17] Y. Akahane *et al.*, Nature (London) **425**, 944 (2003).
[18] H.-G. Park *et al.*, Appl. Phys. Lett. **79**, 3032 (2001).
[19] H. Gersen *et al.*, Phys. Rev. Lett. **94**, 073903 (2005).
[20] Y. A. Vlasov *et al.*, Nature (London) **438**, 65 (2005).
[21] B.-S. Song *et al.*, Nature (London) **4**, 207 (2005).
[22] T. Asano, B.-S. Song, and S. Noda, Opt. Express **14**, 1996
(2006).
[23] P. E. Barclay, K. Srinivasan, M. Borselli, and O. Painter,
Electron. Lett. **39**, 842 (2003).
[24] S. Noda, A. Chutinam, and M. Imada, Nature (London)
407, 608 (2000).
[25] A. Taflove and S. C. Hagness, *Computational Electro-
dynamics: The Finite-Difference Time-Domain Method*
(Artech House, Norwood, MA, 2005).
[26] R. D. Meade *et al.*, Phys. Rev. B **48**, 8434 (1993).
[27] S. Hughes *et al.*, Phys. Rev. Lett. **94**, 033903 (2005).
[28] D. Thouless, Phys. Rev. Lett. **39**, 1167 (1977).
[29] Y. A. Vlasov, M. A. Kaliteevski, and V. V. Nikolaev, Phys.
Rev. B **60**, 1555 (1999).
[30] S. Mookherjea and A. Oh, Opt. Lett. **32**, 289 (2007).